NANOFABRICATION
Research Article • DOI: 10.2478/nanofab-2013-0001 • NANOFAB • 2013 • 1-7

Electroless selective deposition of gold nano-array for silicon nanowires growth

Abstract
Nanopatterns of gold clusters on a large surface of oriented Si(111) substrates, from the galvanic displacement of gold salt (*via* the spontaneous reduction of $AuCl_4^-$), are demonstrated in this work. The Si substrate is patterned by Focused Ion Beam (FIB) prior to being dipped in a gold solution. Here, we show that these patterns lead to successful control of the position and size of gold clusters. Sequential patterning reveals a powerful maskless alternative to surface preparation prior to Si nanowire growth.

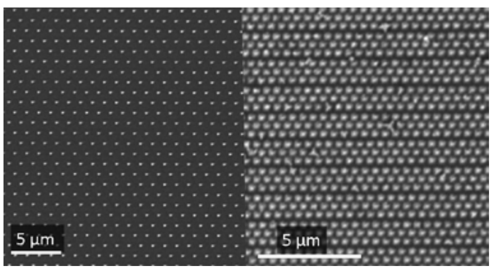

E. Ruiz-Gomes[1,2], C. Herrier[1]*, A. Gouyé[1], A. Benkouider[1], P. Sudraud[2], A. Delobbe[2], A. Ronda[1], I. Berbezier[1]

[1]Institut Matériaux Microélectronique Nanosciences de Provence, UMR CNRS 7334, Aix-Marseille Université, 13397 Marseille Cedex 20, France

[2]Orsay Physics, 13710 Fuveau, France

Keywords
Silicon • Gold • Galvanic displacement • FIB patterning • Lithography • Nanostructures • Nanowires

Received 10 April 2013
Accepted 13 August 2013

1. Introduction

Gold nanoparticles are currently the interest of many studies as it is possible to synthesize particles with different sizes and shapes. Many studies deal with the organization of these particles on surfaces or in volume, in order to obtain nanostructures with unique properties. The good chemical stability of gold, its high conductivity and dimension of the nanostructures offers many applications such as in optical spectroscopy (due to a surface enhanced effect with Plasmon wave) [1,2] or in nanowire growth engineering [3].

Galvanic displacement (GD) is an easy and efficient approach to deposit metallic layers on a conductive substrate [4] and is compatible with various lithographic processes [5,6]. The reaction is fast, spontaneous and occurs at room temperature with less constraints than evaporation or sputtering processes [7]. Previous studies have shown epitaxial growth of gold islands during electrochemical processes [8,9] Further, metal deposition occurs on conductive and semi-conductive surfaces but not on insulating surfaces [10-13]. This specificity allows an oxide layer to be used as a mask to control metal localization on complex micro-architectures [14].

The natural selectivity of GD allows it to be used for a bottom-up approach to surface patterning. In the present study, we combine this technique with a sequential method of nanostructuring based on Focused Ion Beam (FIB) lithography which can be used to draw any desired pattern.

In the first part of this work we briefly describe gold deposition through the galvanic displacement process followed by a discussion of the effect of FIB patterning of the substrate and of a thermally oxidized layer on the substrate for the localisation of gold drops. Finally, we present the use of a gold ad-hoc nanoarray for ordering Si nanowires growth.

2. Experimental Procedure

The samples used in this study are Si(111) substrates with or without oxide layers. The sample preparation consists of a two or three step process depending on the substrate used.

First, a thermal oxide layer (SiO_2) is formed on a silicon substrate; the surface is cleaned beforehand with a chemical cleaning procedure (RCA and Shiraki) to obtain a surface cleared of impurities. Thermal oxide was formed with a rapid thermal

* E-mail: cyril.herrier@cea.fr

annealing (from JIPELEC): 5 minutes at 1000°C under O_2 flow which allows growing a 5 nm thick oxide film.

The second step consists of performing patterns in the SiO_2 film (Oxide layer must be crossed to reach Si, as gold does not stick on SiO_2). The objective is to use the oxide film as a mask to organize gold drops. Patterning experiments have been carried out using a COBRA Focused Ions Beam (FIB) from Orsayphysics coupled to a Scanning Electron Beam (SEM) from Tescan; this dual beam allows simultaneous electron imaging and ion patterning. COBRA-FIB also provides a liquid metal ions source (LMIS) and liquid metal ions alloy source (LMIAS) thanks to a Wien filter which separates the different elements according to their mass. For this work, LMIS was used as Ga^+ source;the ions acceleration energy can be varied between 5 to 30 keV.

Several arrays of nanopatterns (holes) have been milled. The nanopatterns' size, depth and aspect ratio were changed by varying the ion beam current, ion dose, dwell time and spot size. The amount of Ga^+ ions that irradiate the sample depends on each one of these parameters. The periodicity of patterns was chosen at 1 µm for lines and dots and the dose was of 2.5 x 10^{15} ions cm^{-2} s^{-1}. Under these conditions we obtained a minimal resolution of 50 nm for the pattern. The sputtering angle between the ion beam and the Si substrate surface was kept constant at 90° (normal incidence).

In a final step, gold is deposited onto FIB patterns by galvanic displacement (GD), *i.e.* the spontaneous reduction of $AuCl_4^-$ on silicon surface. Before this deposition, the sample was dipped in 0.25% hydrofluoric (HF) aqueous solution for 2 minutes to remove the native oxide potentially present at the bottom of the holes. GD was used in two ways: 1) "non-limited", which consists of dipping the sample into an aqueous solution containing $HAuCl_4$ (0.1% - from Sigma) and HF (0.1%) and 2) "self-limited", which consists of using a solution without any HF but only gold salt. Samples are finally copiously rinsed with ultra-pure water (Millipore) then dried under N2 blow.

Atomic Force Microscopy (AFM) topography was used to characterize gold deposition on the homogeneous surface. Scanning Electron Microscopy (with secondary and backscattering electrons) was used to control gold particles position.

3. Results and Discussion

In order to study surface effects on deposited gold, three different samples were used: 1) hydrogenated silicon substrate without FIB, 2) hydrogenated silicon substrate with FIB and 3) silicon with patterned thermal oxide.

3.1 Hydrogenated silicon surface without FIB

Galvanic displacement deposition of gold is usually performed in a fluorinated solution in order to simultaneously dissolve oxide silicon due to gold-salt reduction [15]. This reaction can also occur without addition of HF and is known as "self-limited deposition" [16]. In the first case, a topographic picture shows a continuous film of gold with roughness of few nm (Figure 1); the time of reaction determines the gold quantity on the surface.

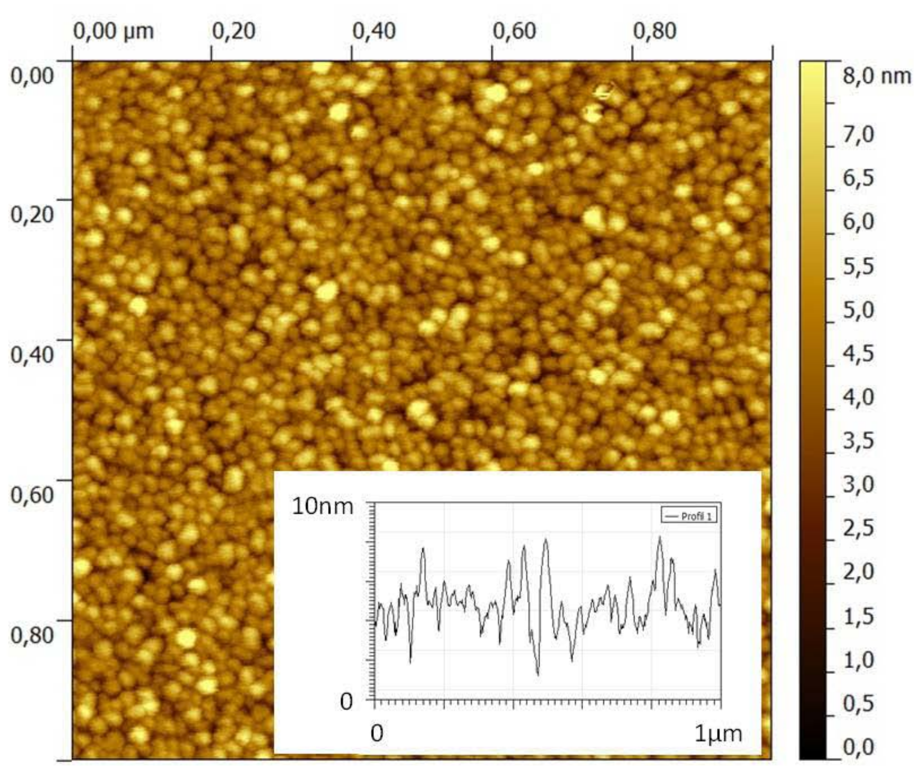

Figure 1. AFM topography of Si(111) hydrogenated surface dipped 5min in $HAuCl_4$ solution with 0,25%HF – Inset: topography profile.

In the second case, topographic pictures show nanoparticles of gold. After dipping the surface with self-limited deposition in HF solution, less particles are present (Figure 2); these images show that some particles stay on pure silicon and are not removed during oxide dissolving.

3.2 Hydrogenated silicon surface milled by focused ions beam

Ga FIB milling of hydrogenated silicon surface allows for gold deposition control. Implanted areas can be used to limit gold deposition directly on the Si surface (without oxide) while allowing to localize gold clusters (Figure 3). Dots and line patterns were performed with 1 µm step and 2.5 x 10^{15} ions cm^{-2} s^{-1}.

Outside the FIB pattern, the surface is covered with gold droplets. Alternatively, FIB patterns are without gold which is only present between dots or lines. This phenomenon seems to be clearly related to the presence of Ga. Removing Ga by thermal and HCl treatment allows more gold in and between FIB milling as shown in Figure 4.

In order to deposit gold exclusively in the patterns, we suggest using a silicon oxide layer as a trap for Ga atoms.

3.3 Oxide layer structuration

Figure 5 shows a non-limited gold deposition on four hexagonal dot patterns prepared on silicon oxide with different doses. The change in contrast as result of SEM analysis, allows estimating of the amount of gold deposited in FIB milling; despite this selective process gold is still present outside the patterns. These results can be explained by simultaneous gold deposition and oxide dissolution.

To reduce undirected gold deposition we use the self-limited alternative of GD (*i.e.* without HF during metal deposition). A brief dipping in highly diluted HF prior to deposition avoids a thin native oxide layer in the bottom of holes. This increase of selectivity with a silicon oxide layer used as a mask for galvanic deposition of gold has been previously described [17].

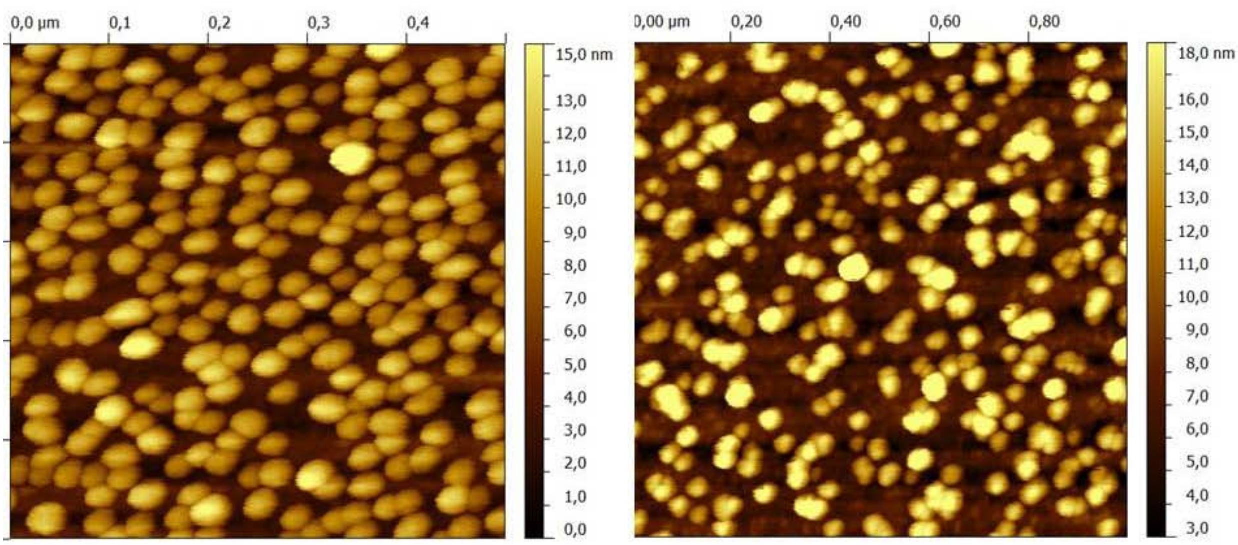

Figure 2. *left: AFM topography of Si(111) hydrogenated surface dipped 5min in $HAuCl_4$ solution without HF – right: same surface after 2min dipping in 4% HF*

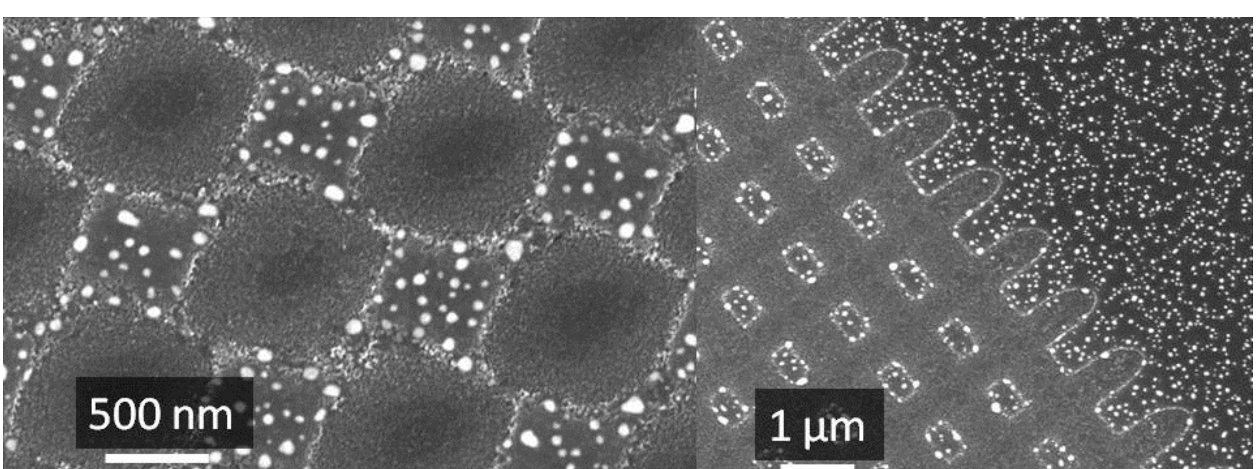

Figure 3. *SEM image of dots pattern (a) and lines pattern (b). Gold deposition is by GD with a no-limiting way.*

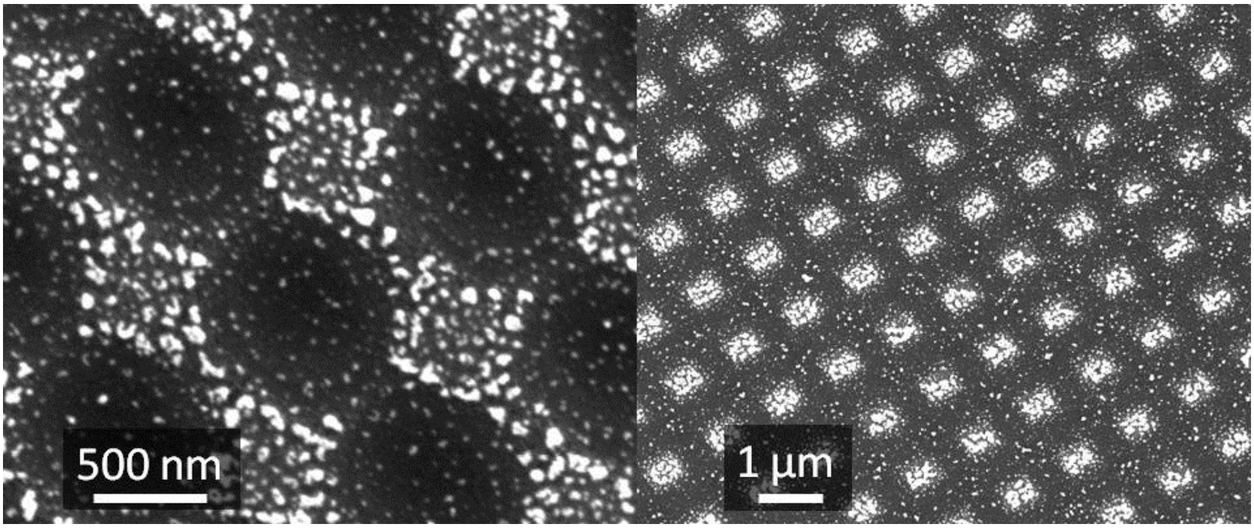

Figure 4. *Gold deposition by GD on the same pattern as figure 3. Ga atoms implanted in the surface were removed before gold deposition.*

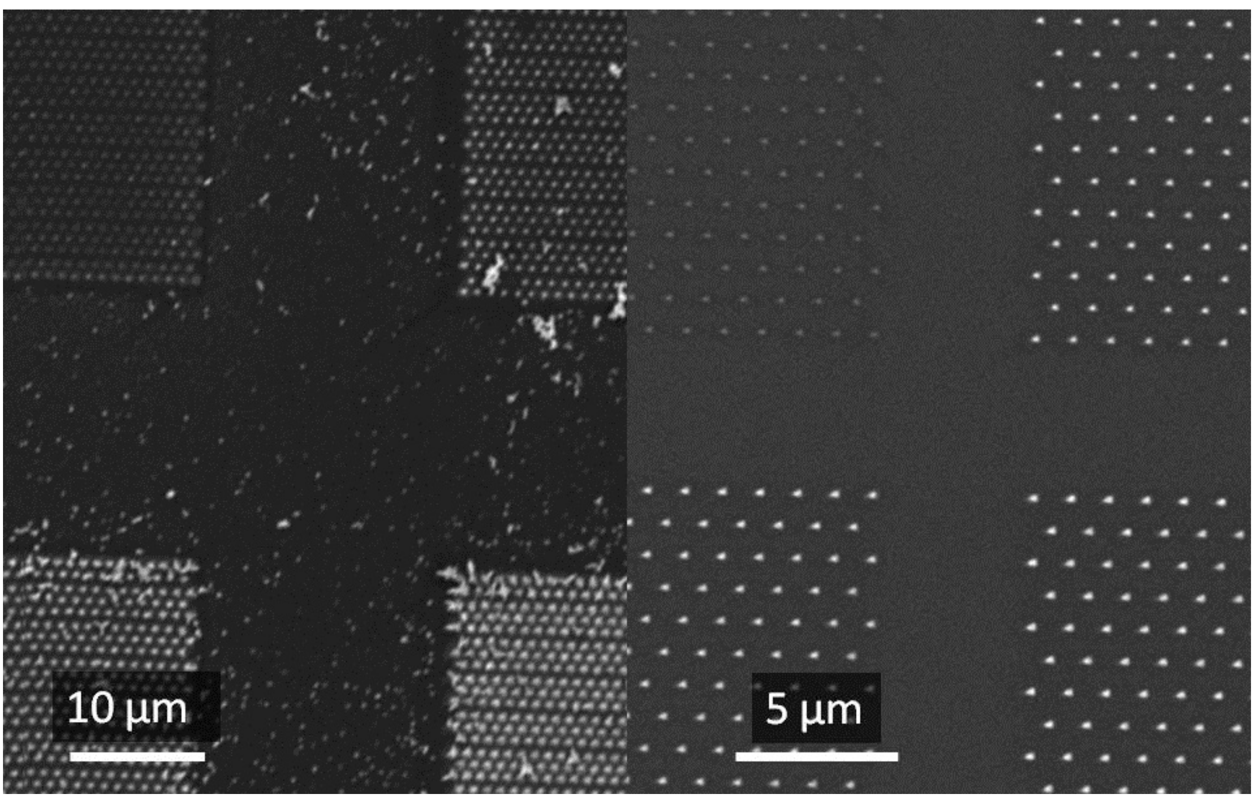

Figure 5. *SEM of thermal oxide silicon surface patterned by FIB then dipped 5min in $HAuCl_4$ solution with 0.25%HF (left) and without HF (right). Increasing FIB dose was employed to mill the patterns in the four corner of pictures.*

Final dipping in HF results in an H-terminated silicon surface with organized nano-clusters of gold directly bound to Si (Figure 5).

3.4 Discussion

A galvanic displacement reaction is a spontaneous electrochemical mechanism which occurs where there is a large difference between the redox potential of species (Figure 6). AFM and SEM images show the granular character of the deposition (Insets Figure 7). Initially, galvanic displacement leads to the growth of gold clusters. A non-limited process leads to a very smooth surface (Figure 1), while a few minutes of self-limited GD leads to individual particles of 5 nm heights with a surface coverage of average 75% (Figure 2 left). Gold particles

$$AuCl_4^- + 3\,e^- \rightarrow Au(s) + 4\,Cl^- \qquad E^0_{Au3+/Au} = 0.94 \text{ V vs SHE}$$

$$Si(s) + 6\,F^- \rightarrow SiF_6^{2-} + 4\,e^- \qquad E^0_{SiF6\,2-/Si} = -1.68 \text{ V vs SHE}$$

$$SiO_2(s) + 2\,H_2O \rightarrow SiO_2(s) + 4\,H^+ + 4\,e^- \qquad E^0_{SiO2/Si} = -1.15 \text{ V vs SHE}$$

Figure 6. Redox potential of cathodic and anodic reactions that occur in the galvanic displacement of aurate.

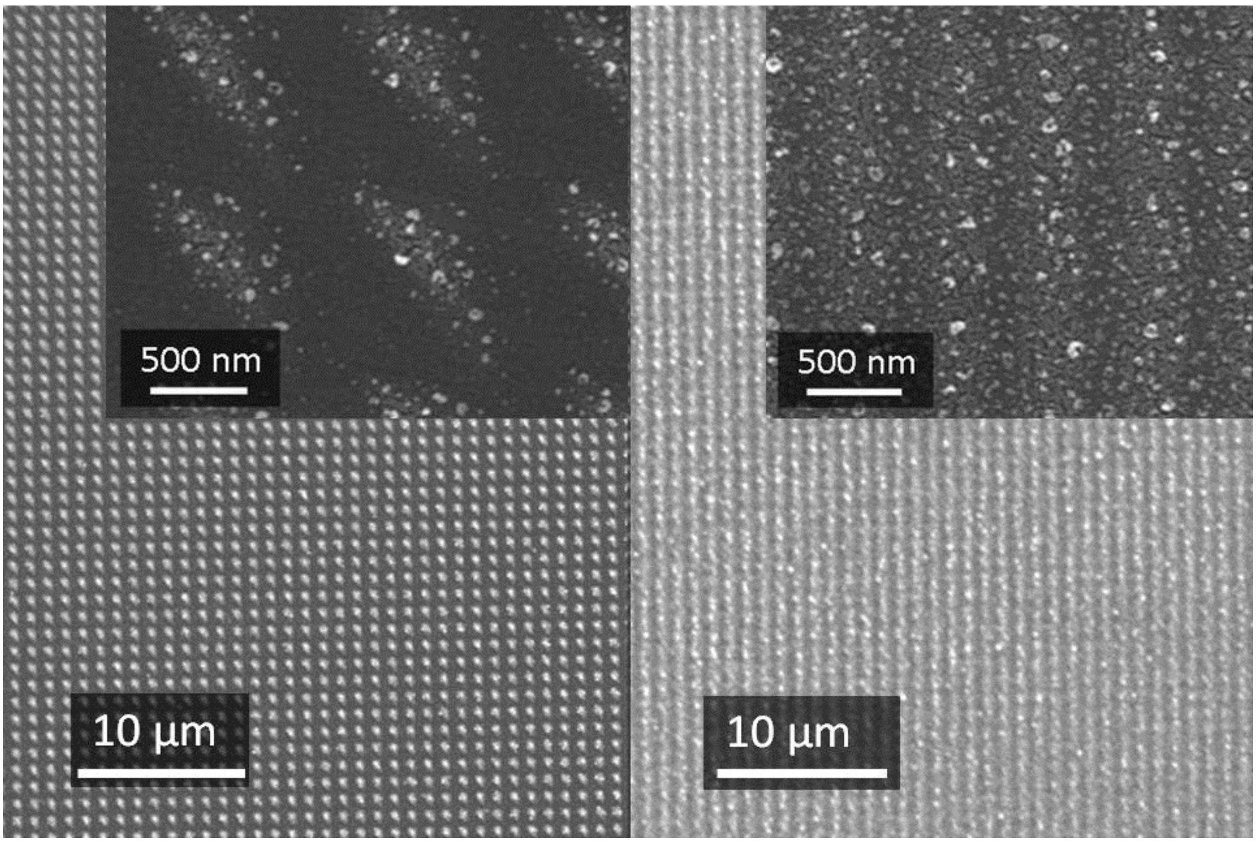

Figure 7. SEM of thermal oxide silicon surface patterned by FIB then dipped 5 min in $HAuCl_4$ solution without HF – pattern pitch = 1 µm (left) or 500 nm (right). Insets are high-resolution images.

stay on the surface after a HF dipping (60% of surface coverage – Figure 2 right); this is made possible due to direct deposition of gold on Silicon which indicates that the anodic oxide formation is separate from a few nanometers to the cathodic site. At the anode, Si atoms are rapidly oxidized by O atoms from dissolved O_2 and water. A separation between the cathodic and anodic site is typical in metals. However, in semiconductors, the length of separation of these sites is limited by the conductivity. Further, gold layers are well known to grow following Volmer-Weber mode [18,19] which favors lateral expansion but can be limited by the silicon oxide resulting from the reduction of aurate. A minimal pitch depth of average 500 nm has been observed for which growing gold clusters merge (Figure 7). Larger gold drops can be obtained by heating the samples to 600 °C. At this temperature, gold dewetting occurs and forms patterned droplets on structured substrates (Figure 8). Thus, gold densification can be

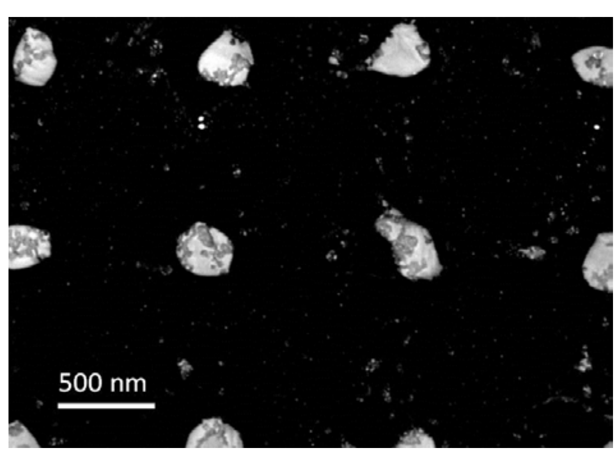

Figure 8. SEM gold drops after heating up selective gold deposit on structured substrate.

achieved by successive dipping in highly diluted HF and gold salt deposition.

The sequential FIB process allows ad-hoc structures with nanoscale resolution, which can be used in various technologies (Supporting Information), to be obtained. Sequential top-down structuration followed by full-wafer metal deposition combines the versatility of top-down approaches with the spontaneity and speed of a bottom-up process. Making a template on large surface with self-assembly methods can also be compatible with GD to obtain very large nanopatterns [20-22].

Au drops on Si substrate [7] are used for Si nanowire (NW) growing. SiNWs growth *via* a vapor-liquid-solid mechanism [23,24] and can be implemented in CVD [21,22] or MBE [25]. MBE allows precise control over growth rates, which we expect to lead to a greater degree of control of the SiNWs shapes. First, results with homogeneous substrates lead to NWs with very different sizes and shapes (Figure 9). We managed to use gold patterns to grow SiNWs with a MBE process which must be improved (Figure 10). Controlling the position and size of gold droplets, which are used as seed, can allow engineering position and shapes of NWs [25-28].

4. Conclusions

This study reports FIB structuring of silicon wafers in order to precisely control the position and size of gold clusters. We achieved placement of groups of gold particles of hundreds nanometers in width with a lateral resolution of half of a micrometer. Patterns milled by FIB have a lateral resolution 50 nm on average.

Controlling the metal deposition [29,30] on a conductor or semiconductor is of interest for further controlled crystalline growth of nanomaterials [31], improving electrocatalytic performance [6], and also for optical sensors [32].

Aknowledgements

E.G. thanks Orsay Physics for PhD grant.

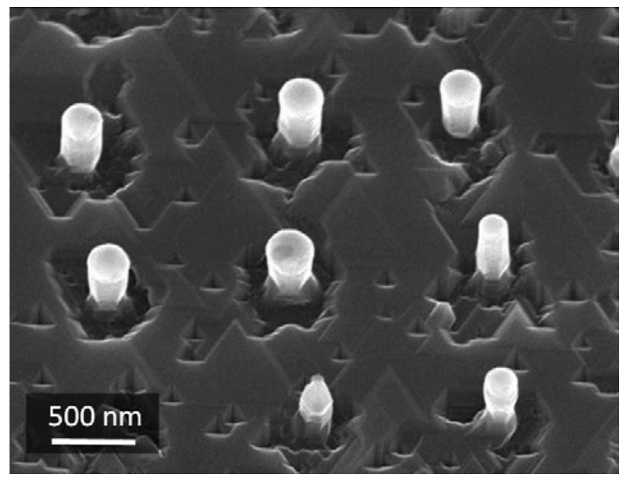

Figure 10. *SEM of Silicon nanowire patterns grown by MBE from gold patterns obtained by the method illustrated in this study.*

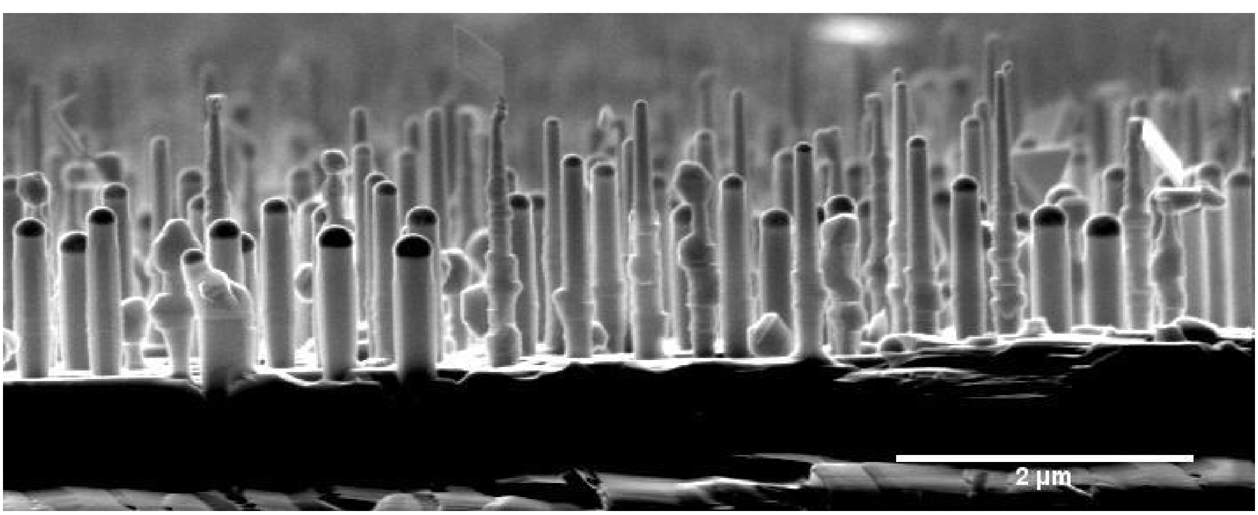

Figure 9. *SEM cross-section of Si nonawires grown by MBE on an initially uniform gold coverage of a non-patterned silicon surface.*

References

[1] Stewart, M. E. et al. Chem. Rev. 108, 494 (2008).

[2] Campion, A. & Kambhampati, P. Chem. Soc. Rev. 27, 241 (1998).

[3] Chou, Y.-C. et al. ACS Nano 6, 6407 (2012).

[4] Magagnin, L., Maboudian, R. & Carraro, C. J. Phys. Chem. B 106, 401 (2002).

[5] Porter, L. A. et al. Nano Letters 2, 1369 (2002).

[6] Fabre, B., Hennous, L., Ababou-Girard, S. & Meriadec, C. ACS appl. Mat. Int. 5, 338 (2013).

[7] Piscopiello, E. et al. Phys. Rev. B 78, 035305 (2008).

[8] Warren, S. et al. Surf. Sci. 496, 287 (2002).

[9] Sayed, S. Y. et al. ACS nano 3, 2809 (2009).
[10] Sugimura, H. & Nakagiri, N. Appl. Phys. Lett. 66, 1430 (1995).
[11] Carraro, C., Magagnin, L. & Maboudian, R. Electrochimica Acta 47, 2583 (2002).
[12] Magagnin, L., Bertani, V., Cavallotti, P. L., Maboudian, R. & Carraro, Microelec. Eng. 64, 479 (2002).
[13] Fabre, B. & Herrier, C. RSC Advances 2, 168 (2012).
[14] Carraro, C., Maboudian, R. & Magagnin, L. Surf. Sci. Rep. 62, 499 (2007).
[15] Srinivasan, R. Kinetic J. Electrochem. Soc. 146, 570 (1999).
[16] Gutés, A., Carraro, C. & Maboudian, R. ACS appl. Mat. Int. 3, 1581 (2011).
[17] Kimin Jun, and Joseph M. Nano Lett. 10, 2777–2782 (2010).
[18] Blackman, J. A. & Wilding, A. Europhysics Letters 16, 115 (1991).
[19] Ji, C., Oskam, G. & Searson, P. C. Surf. Sci. 492, 115 (2001).
[20] Aizawa, M. & Buriak, J. M. JACS 127, 8932 (2005).
[21] Shimizu, T., Senz, S., Shingubara, S. & Gösele, U. Appl. Phys. A 87, 607 (2007).
[22] Shimizu, T. et al. Adv. Mat. 19, 917 (2007).
[23] Wagner, R. S. & Ellis, W. C. Appl. Phys. Lett. 4, 89 (1964).
[24] Wu, Y. & Yang, P. JACS 123, 3165 (2001).
[25] Marcus, I. C. et al. Crystal Growth & Design 11, 3190 (2011).
[26] Cui, Y., Lauhon, L. J., Gudiksen, M. S., Wang, J. & Lieber, C. M. Appl. Phys. Lett. 78, 2214 (2001).
[27] Gao, D. et al. JACS 127, 4574 (2005).
[28] Tseng, C.-H., Tambe, M. J., Lim, S. K., Smith, M. J. & Gradečak, S. Nanotechnology 21, 165605 (2010).
[29] Cerruti, M., Doerk, G., Hernandez, G., Carraro, C. & Maboudian, R. Langmuir 26, 432 (2010).
[30] Magagnin, L., Maboudian, R. & Carraro, C. Electrochemical and Solid-State Letters 4, C5 (2001).
[31] Paulo, A. S. et al. Nano letters 7, 1100–4 (2007).
[32] Hutter, E. & Fendler, J. H. Adv. Mat. 16, 1685–1706 (2004).